A POWERFUL SUPERVISED FUZZY METHOD. CHARACTERIZATION, AUTHENTICATION AND TRACEABILITY OF ROMAN POTTERY

HORIA F. POP[a], COSTEL SÂRBU[b*]

ABSTRACT. A supervised fuzzy method is described and efficiently applied for the first time in this study. The advantages of the new approach for the characterization and classification of various Roman potteries on the basis of their mineral composition has been explored. The new classification robust approach allows more relevant conclusions to be drawn, finding more specific groups and a better characterization of Roman potteries using their degrees of membership to each fuzzy partition and solving in this way some discrepancies. The efficiency of the supervised fuzzy method was also estimated by the values of quality performance features obtained applying different fuzzy quality criteria and highly illustrative graphs. The parameters of the prototype (class centre) illustrate much better than, for example, arithmetic mean the specific characteristics of each class, and the degrees of membership allow a rationale comparison of the similarity and differences of Roman pottery samples investigated.

Keywords: supervised fuzzy method, prototypes, fuzzy quality criteria, Roman pottery, spectrometry

INTRODUCTION

It is well known and widely accepted that data analysis (data science) has reached a new level when chemometric methods have been starting to be efficiently applied [1-5]. These methods offer the best alternative for graphical visualization or finding the natural existing groups and relationships between objects (samples, cases) and/or their characteristics (variables). The most commonly used methods are cluster analysis (CA), principal component analysis (PCA), discriminant analysis (DA), and others more or less sophisticated methods [6-8].

[a] *Department of Computer Science, Faculty of Mathematics and Computer Science, Babeş-Bolyai University, 400084-Cluj-Napoca, Romania*
[b] *Department of Chemistry, Faculty of Chemistry and Chemical Engineering, Babeş-Bolyai University, 400084-Cluj-Napoca, Romania*
* *Corresponding author: costelsarbu@ubbcluj.ro*

Cluster analysis and classification are two important tasks which occur daily in everyday life. The goal of cluster analysis is to find meaningful groups in data [9]. Generally two types of algorithm are distinguished, these being hierarchical and non-hierarchical or relocation (partitioning) clustering. Both methods require the calculation of a (dis)similarity matrix. This (dis)similarity which is really a measure of the proximity of the pair of objects (points) in the p-dimensional characteristic space, defined by the p properties measured for each individual, is usually expressed in terms of the Euclidean, Mahalanobis, Manhattan or Chebychev distance between the two points. Either the number of clusters to be generated can be specified in advance, or it may be optimized by the algorithm itself according to certain criteria.

The problem of classification (also called discriminant analysis) involves classifying objects into classes when there is already information about the nature of the classes. This information often comes from a data set of objects that have already been classified by experts or by other means. Classification aims to determine which class new objects belong to and develops automatic algorithms for doing so. Typically, this involves assigning new observations to the class whose objects they most closely resemble in some sense [7].

Classification is said to be a "supervised" problem in the sense that it requires the supervision of experts to provide some examples of the classes. Clustering, in contrast, aims to divide a set of objects into groups without any examples of the "true" classes, and so is said to be an "unsupervised" problem [7].

In classical cluster analysis and classification each object must be assigned to exactly one cluster or class. This is a source of ambiguity and error in cases of outliers or overlapping clusters and affords a loss of information. This kind of vagueness and uncertainty can, however, be taken into account by using the theory of fuzzy sets [10]. A fuzzy set or a fuzzy subset is a collection of ill-defined and not-distinct objects with un-sharp boundaries in which the transition from membership to non-membership in a subset of a reference set is gradual rather than abrupt.

The theory of fuzzy set is basically a theory of graded concepts. It is an extreme generalization of ordinary set theory [11] and is basically designed to handle the concept of partial truth. A central concept of fuzzy set theory is that it is permissible for an element to belong partly to a fuzzy set. It provides an adequate conceptual framework as well as a powerful mathematical tool to model the real-world problems which are often obscure and indistinct [12-16].

The data arising from fuzzy systems are in general, soft, with no precise boundaries. Fuzziness of this type can often be used to represent situations in the real world better than the rigorous definitions of crisp set

theory [11]. Fuzzy sets can be particularly useful when dealing with imprecise statements, ill-defined data, incomplete observations or inexact reasoning. There is often fuzziness in our everyday world as, for example, varying signal heights in spectra from the same substance, or varying patterns in pattern recognition studies [12-16].

The goal of the present study is to define and apply a new methodology for Roman potteries characterization and classification, improving in this way the approach proposed by Mirti and al. [17]. The new classification robust approach used here allows more relevant conclusions to be drawn, finding more specific groups and a better characterization of Roman potteries using their degrees of membership to each fuzzy partition and solving in this way some discrepancies. The efficiency of the supervised fuzzy method was also estimated by the values of quality performance features obtained applying different fuzzy quality criteria [13, 18, 19] and highly illustrative graphs.

RESULTS AND DISCUSSION

Step 1. First we started to run the data set including 16 samples (training set) accurately assigned to three groups (according to their stylistic features and results obtained using different multivariate methods applied to spectroscopic data) as the authors of the original study indicated [17]. The input and output partitions, namely the degrees of membership (DOMs), are shown in Table 1. The supervised fuzzy c-means (SFCM) produced 3 fuzzy partitions (groups), which were all represented by a prototype (a cluster centre with the parameters corresponding to the fuzzy robust means of the original spectral concentrations for 16 terra sigillata samples weighted by DOMs corresponding to each partition). To compare the fuzzy partitions and the similarity and differences of samples, we have to analyse both the characteristics of the prototypes corresponding to the three fuzzy partitions (A1–A3) obtained by applying SFCM and DOMs of samples corresponding to all fuzzy partitions. The results presented in Table 1 and 2 and also Figure 1 clearly illustrate the most specific characteristics of each fuzzy partition and their (dis)similarity and point out the samples assigned according to their DOMs.

The fuzzy partition A1, for example, has a moderate concentration of Al (18.25%) but the highest concentration of Fe (8.87%) and Mg (7.85%) and the smallest concentration of Ca (2.46%). This partition contains all the samples assigned by Mirti and al. [17] to the group I with very high DOMs within the range 0.964-0.997.

Table 1. The input and output partitions (DOMs) of the training set (n=16)

No	Symbol	Site	Position	Input partitions			Output partitions		
				A1	A2	A3	A1	A2	A3
1	A2	PPS	N-W	1	0	0	**0.977**	0.010	0.013
2	A8	PPS	N-W	1	0	0	**0.964**	0.017	0.020
3	A8b	PPS	N-W	1	0	0	**0.997**	0.001	0.002
4	B1	PPS	N or C	0	0	1	0.019	0.038	**0.944**
5	B4	PPS	N-W	1	0	0	**0.995**	0.002	0.003
6	B12	PPS	N-W	1	0	0	**0.987**	0.006	0.007
7	B13	PPS	N-W	1	0	0	**0.979**	0.009	0.012
8	B14	PPS	N-W	1	0	0	**0.985**	0.006	0.009
9	B15	PPS	N or C	0	0	1	0.049	0.141	**0.810**
10	B21	PPS	N or C	0	0	1	0.023	0.058	**0.919**
11	W2	PP	G	0	1	0	0.095	0.206	**0.700**
12	W3	PP	G	0	1	0	0.006	**0.972**	0.022
13	W4	PP	G	0	1	0	0.010	**0.955**	0.035
14	W5	PP	G	0	1	0	0.036	0.115	**0.849**
15	W6a	PP	G	0	1	0	0.008	**0.962**	0.030
16	W6b	PP	G	0	1	0	0.030	0.126	**0.844**

PPS= Porta principalis sinistra; PP= Porta Praetoria;
G= Gaulish production; N-W= north-western; N or C= north or central

Table 2. The coordinates (fuzzy means) of the prototypes
corresponding to different partitions (%)

Partition	Al_2O_3	Fe_2O_3	CaO	MgO	Na_2O	K_2O	TiO_2	MnO
n = 16								
A1	18.25	8.87	2.46	7.85	1.61	3.71	0.98	0.13
A2	21.58	5.81	9.98	1.16	0.14	3.88	0.80	0.07
A3	16.52	6.70	10.54	3.25	1.00	3.06	0.83	0.13
n = 21								
A1	18.41	8.92	2.40	8.10	1.54	3.65	0.92	0.13
A2	21.41	5.80	9.64	1.20	0.17	3.82	0.82	0.07
A3	16.54	6.66	10.27	3.21	0.99	3.03	0.84	0.13
n = 24								
A1	19.61	8.04	2.76	5.74	1.39	3.34	0.85	0.11
A2	20.74	5.74	5.40	1.56	0.76	3.29	0.78	0.06
A3	14.91	6.28	11.88	2.99	0.87	2.92	0.73	0.11

The fuzzy partition A2, with the highest concentration for Al (21.58%), and also a high concentration for Ca (9.98%) but with the smallest concentration for Fe (5.81%), Mg (1.16%) and Na (0.14%), includes only three samples from the group II, as it was indicated by Mirti and al. [17], namely W3, W4 and W6a with the following very high DOMs: 0.972, 0.955 and 0.962. The other three samples namely W2, W5 and W6b were assigned to A3 with relatively high DOMs: W2 (0.700), W5 (0.849) and W6b (0.844).

The fuzzy partition A3 includes the three samples moved from A2 and the three samples B1 (0.944), B15 (0.810) and B21 (0.919) assigned to group III by Mirti and al. [17]. This partition is characterized by the highest concentration of Ca (10.54%), the smallest concentration of Al (16.52%) and the intermediate concentration for Fe (6.70%) and Mg (3.25%).
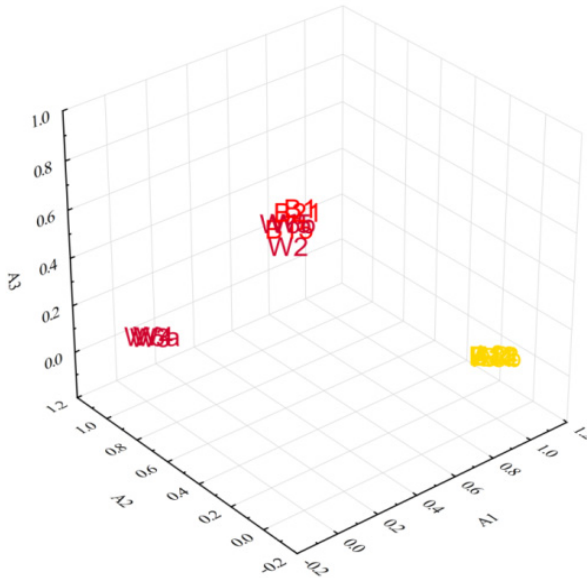

Figure 1. 3-D scatterplot of DOMs corresponding to A1, A2 and A3 (n = 16)

All of the above statements concerning the efficiency of SFCM are well supported also by 2D and 3D scatterplot of DOMs corresponding to the three partitions (very compact groups) (Figure 1) and the values of the fuzzy clustering validity indices considered (Table 3): partition coefficient-PC (optimal/ maximum value = 1); partition entropy-PE (optimal/minimum value = 0); Backer-Jain index-BJI (optimal/maximum value = 1) and Xie-Beni index-XBI (optimal/minimum value = 0).

Table 3. The clustering validity indices values

Fuzzy partition	Clustering validity index			
	PC	PE	BJI	XBI
n = 16	0.8739	0.2604	0.9071	0.0623
n = 21	0.8329	0.3277	0.8506	0.1415
n = 5	0.7016	0.5429	0.6701	0.3702
n = 45	0.6792	0.5660	0.7101	0.4381
n = 24	0.5448	0.7743	0.5872	0.3555

Step 2. Considering now the results obtained at the first step we will use the output partition of the training set as an input partition to predict the assignments of the five uncertain samples indicated in Table 4 and Table 5. All five samples are assigned to A1 but with quite different DOMs: B2 (0.985), Wla (0.927), Wlb (0.911), B3 (0.671) and B16 (0.381). The case of B16 is quite interesting because its DOMs to the three partitions are practically equal, and this aspect illustrates in fact a large difference of B16 from the samples assigned to A1, A2 and A3 with very high DOMs (Table 4 and Figure 2). We have to remark also the slight modification of the characteristics of prototypes and the values of fuzzy clustering validity indices (n = 21) comparing with data corresponding to the training data set (n = 16), presented also in Table 2 and 3.
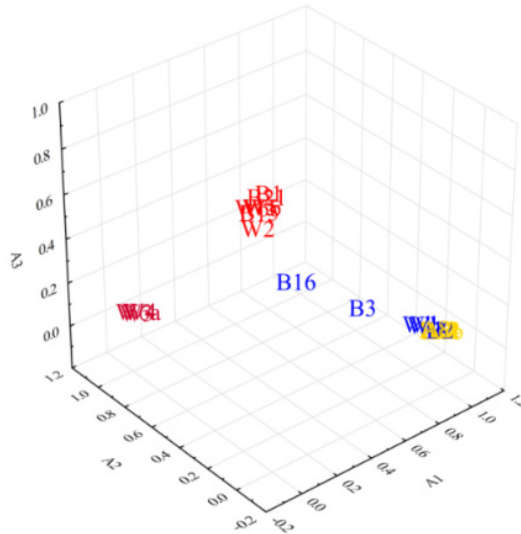

Figure 2. 3-D scatterplot of DOMs corresponding to A1, A2 and A3 (n = 21)

Table 4. The input and output partitions of the predicting set (n=21)

No	S*	Site	P*	Input partitions			Output partitions		
				A1	A2	A3	A1	A2	A3
1	A2	PPS	N-W	**0.977**	0.010	0.013	**0.977**	0.010	0.013
2	A8	PPS	N-W	**0.964**	0.017	0.019	**0.964**	0.017	0.019
3	A8b	PPS	N-W	**0.997**	0.001	0.001	**0.997**	0.001	0.002
4	B1	PPS	N or C	0.019	0.038	**0.943**	0.019	0.038	**0.944**
5	B4	PPS	N-W	**0.995**	0.002	0.004	**0.995**	0.002	0.003
6	B12	PPS	N-W	**0.987**	0.006	0.007	**0.987**	0.006	0.007
7	B13	PPS	N-W	**0.979**	0.009	0.012	**0.979**	0.009	0.012
8	B14	PPS	N-W	**0.985**	0.006	0.009	**0.985**	0.006	0.009
9	B15	PPS	N or C	0.049	0.141	**0.810**	0.049	0.141	**0.810**
10	B21	PPS	N or C	0.023	0.058	**0.919**	0.023	0.058	**0.919**
11	W2	PP	G	0.095	0.205	**0.700**	0.095	0.206	**0.700**
12	W3	PP	G	0.006	**0.972**	0.022	0.006	**0.972**	0.022
13	W4	PP	G	0.010	**0.955**	0.035	0.010	**0.955**	0.035
14	W5	PP	G	0.036	0.115	**0.849**	0.036	0.115	**0.849**
15	W6a	PP	G	0.008	**0.961**	0.030	0.008	**0.962**	0.030
16	W6b	PP	G	0.030	0.126	**0.844**	0.030	0.126	**0.844**
17	B2	PPS	?	-	-	-	**0.985**	0.007	0.008
18	B3	PPS	?	-	-	-	**0.671**	*0.177*	*0.152*
19	B16	PPS	?	-	-	-	**0.381**	*0.293*	*0.326*
20	Wla	PP	?	-	-	-	**0.927**	0.031	0.042
21	Wlb	PP	?	-	-	-	**0.911**	0.041	0.048

Symbol; PPS= Porta principalis sinistra; PP= Porta Praetoria; G= Gaulish production; N-W= north-western; N or C= north or central; ? = uncertain; P= position

Step 3. In order to identify the origin of the 24 common ware samples, we used the results obtained at step 1 and 2 as input partition presented in Table 5 and the spectral data. The final results are shown in Table 5. Considering the DOMs of the 24 samples to the three partitions the following conclusions can be formulated. Six common ware samples are assigned to partition A1, four with relatively high DOMs: A3 (0.878), B5 (0.701), B18 (0.886), B19 (0.767), and two samples with small DOMs: B11 (0.531) and B20 (0.571). Thirteen samples (A6, A7, A9, A10, A11, A12, A13, B8, B9, B10, B22, B23, B24) are assigned to partition A2 with relatively small and quite similar DOMs within the range (0.501-0.685). Five samples (A4, A5, B6, B7, B17) are assigned to partition A3 with relatively high DOMs within the range (0.744-0.911). The similarity and differences of the considered common wares with terra sigillata is also well illustrated in Figure 3.

Table 5. The input and output partitions of the predicting set (n = 45)

No	S*	Site	P*	Input partitions			Output partitions		
				A1	A2	A3	A1	A2	A3
1	A2	PPS	N-W	**0.977**	0.010	0.013	**0.977**	0.010	0.013
2	A8	PPS	N-W	**0.964**	0.017	0.019	**0.964**	0.017	0.019
3	A8b	PPS	N-W	**0.997**	0.001	0.002	**0.997**	0.001	0.002
4	B1	PPS	N or C	0.019	0.038	**0.944**	0.019	0.038	**0.944**
5	B4	PPS	N-W	**0.995**	0.002	0.003	**0.995**	0.002	0.003
6	B12	PPS	N-W	**0.987**	0.006	0.007	**0.987**	0.006	0.007
7	B13	PPS	N-W	**0.979**	0.009	0.012	**0.979**	0.009	0.012
8	B14	PPS	N-W	**0.985**	0.006	0.009	**0.985**	0.006	0.009
9	B15	PPS	N or C	0.049	0.141	**0.810**	0.049	0.141	**0.810**
10	B21	PPS	N or C	0.023	0.058	**0.919**	0.023	0.058	**0.919**
11	W2	PP	G	0.095	0.205	**0.700**	0.095	0.206	**0.700**
12	W3	PP	G	0.006	**0.972**	0.022	0.006	**0.972**	0.022
13	W4	PP	G	0.010	**0.955**	0.035	0.010	**0.955**	0.035
14	W5	PP	G	0.036	0.115	**0.849**	0.036	0.115	**0.849**
15	W6a	PP	G	0.008	**0.962**	0.030	0.008	**0.962**	0.030
16	W6b	PP	G	0.030	0.126	**0.844**	0.030	0.126	**0.844**
17	B2	PPS	?	**0.985**	0.007	0.008	**0.985**	0.007	0.008
18	B3	PPS	?	**0.671**	*0.177*	*0.152*	**0.671**	*0.177*	*0.152*
19	B16	PPS	?	**0.381**	*0.293*	*0.326*	**0.380**	*0.293*	*0.326*
20	Wla	PP	?	**0.927**	0.031	0.042	**0.927**	0.031	0.042
21	Wlb	PP	?	**0.911**	0.041	0.048	**0.911**	0.041	0.048
22	A3		C	-	-	-	**0.878**	0.095	0.028
23	A4		C	-	-	-	0.037	0.052	**0.911**
24	A5		C	-	-	-	0.132	0.124	**0.744**
25	A6		C	-	-	-	0.291	**0.639**	0.071
26	A7		C	-	-	-	0.252	**0.685**	0.064
27	A9		C	-	-	-	0.310	**0.619**	0.072
28	A10		C	-	-	-	0.307	**0.617**	0.076
29	A11		C	-	-	-	0.352	**0.570**	0.078
30	A12		C	-	-	-	0.292	**0.642**	0.066
31	A13		C	-	-	-	0.325	**0.553**	0.123
32	B5		C	-	-	-	**0.701**	0.249	0.050
33	B6		C	-	-	-	0.087	0.120	**0.793**
34	B7		C	-	-	-	0.064	0.094	**0.842**
35	B8		C	-	-	-	0.305	**0.559**	0.136
36	B9		C	-	-	-	0.264	**0.576**	0.160
37	B10		C	-	-	-	0.285	**0.514**	0.201
38	B11		C	-	-	-	**0.531**	0.420	0.050
39	B17		C	-	-	-	0.095	0.131	**0.774**
40	B18		C	-	-	-	**0.886**	0.087	0.027
41	B19		C	-	-	-	**0.767**	0.177	0.056
42	B20		C	-	-	-	**0.571**	0.361	0.067
43	B22		C	-	-	-	0.322	**0.609**	0.068
44	B23		C	-	-	-	0.316	**0.622**	0.063
45	B24		C	-	-	-	0.351	**0.501**	0.148

S* =Symbol; P* = Position; PPS= Porta principalis sinistra; PP= Porta Praetoria;
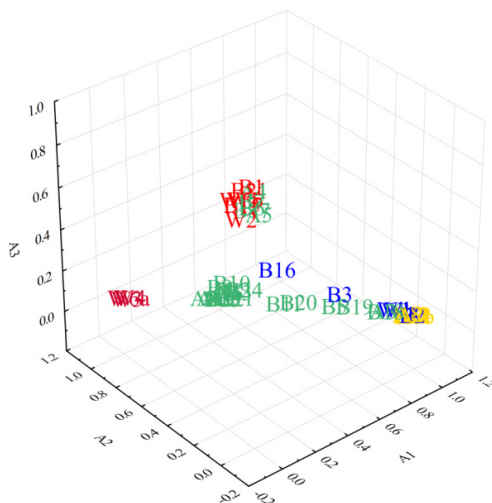G= Gaulish production; N-W= north-western; N or C= north or central

Figure 3. 3-D scatterplot of DOMs corresponding to A1, A2 and A3 (n = 45)

CONCLUSIONS

An advanced chemometric method, namely a robust supervised fuzzy method, has been presented and successfully applied for characterization and classification of 45 Roman potteries according to their chemical composition determined by spectroscopic methods. The obtained results (fuzzy partitions) and parameters of the prototypes (robust fuzzy means) clearly demonstrated the efficiency and information power of this new fuzzy method in Roman potteries characterization and classification and allow a better assignment of samples to a specific group according to their natural origin.

EXPERIMENTAL SECTION

Data sets, analytical and chemometrical methods

In order to prove the highly informative capacity of the new supervised fuzzy method developed and presented here we applied it to an extremely relevant data set discussed by Mirti and al. [17]. The characteristics of 45 sherds excavated within the boundaries of Augusta Praetoria (21 terrae sigillatae and 24 common wares) are presented in Table 5 and their summary chemical composition concerning the percent concentration of 8 metals

determined by spectroscopic methods is shown in Table 2. Pottery represents the most abundant category of portable material culture to come down to us from the Roman world, and it is thus by no means either surprising or inappropriate that pottery studies have enjoyed a position of some prominence in Roman archaeology [23-25]. Terra sigillata pottery is the most famous fine ware of the Roman period. It is characterized by the redness of its body (or paste) and slip (or gloss), similar to the colour of the clay (terra), and by the use of stamps (sigilla) in some cases. Sigillata production can be seen as the industrial activity of specialized workshops. This pottery appeared at first in the mid-first century BC in Italy. Augusta Praetoria (Arezzo) was probably the first important production centre. From the Augustan period (27 BC – 14 AD), sigillata's success had ensured its spread within and outside the Italian Peninsula and branches were established in Pisa and in the south of Gaul. By visual examination of fragments collected at different sites and according to the results obtained applying various multivariate methods, such as hierarchical cluster analysis (HCA), PCA, non-linear mapping (NLM), including also soft independent modelling of class analogy (SIMCA) and K nearest neighbors (KNN), the authors assigned, with more or less accuracy, the majority of considered samples to three main groups. Some discrepancies and uncertain assignments were also mentioned [17].

Supervised fuzzy method

This new method is twofold, composed by a first, learning step and a subsequent prediction step. The underlying assumption is that there is a data set available, previously known and analysed. We are able to construct a fuzzy cluster substructure of that given data set. The method used here might vary, and the assumed cluster shape might vary as well. Once the fuzzy cluster substructure of the given data set is known, the fuzzy partition associated to this data set forms the basis for the prediction step.

Consider a new data set with data items not yet clustered and associated to the fuzzy cluster substructure of the original known data. The purpose of the prediction step is to run a limited fuzzy clustering procedure able to embed these new data items into the fuzzy partition that is already available. At this point, the same method as in the first step is used, but with two major modifications. On one side, all the data items, from both steps, are used in the computation of the class prototypes. On the other side, only the fuzzy membership degrees of the new data items are set and updated along the execution of the method. The fuzzy memberships of the original data items, as computed in the learning step, are kept constant.

Learning step: fuzzify the input classes

Consider a data set $X = \{x^1, \dots, x^n\}$, with $x^j \in \mathbf{R}^s$ for all values of j. Consider a given crisp c-partition of X, (*i.e.,* a partition formed by c classes), where the value of c is predefined. Consider a given fuzziness constant $m > 1$. The purpose of this phase is to fuzzify the input partition and construct a fuzzy c-partition that best corresponds to the cluster structure of the data set. In the particular case of spherical prototypes, this procedure is the Fuzzy c-Means algorithm (FCM) [20,21].

We consider the classes A_i having a particular geometrical shape, and, as such, characterized by a prototype L_i of a certain kind. We are denoting by $D(x^j, L_i)$ the dissimilarity between the data item x^j and the prototype L_i. Depending on the shape of the classes, the dissimilarity D will be defined accordingly.

We aim to minimize the objective function

$$J(P, L) = \sum_{i=1}^{c} \sum_{j=1}^{n} A_i(x^j)^m \cdot D(x^j, L_i).$$

As explained by Bezdek [21], the procedure works by constructing a double Picard iterative process that consecutively minimizes the two functions $J(P, \cdot)$ and $J(\cdot, L)$. The procedure follows:

S1. Set $l = 0$;
S2. Initialize fuzzy partition $P^{(0)} = \{A_1, \dots, A_c\}$ to be the given crisp c-partition of X;
S3. Compute the prototypes L_i that minimize $J(P^{(l)}, \cdot)$;
S4. Compute the fuzzy partition $P^{(l+1)}$ that minimizes $J(\cdot, L)$, as follows:

$$A_i^{(l+1)}(x^j) = \frac{1}{\sum_{k=1}^{c} \left(\dfrac{D(x^j, L_i)}{D(x^j, L_k)} \right)^{\frac{1}{m-1}}};$$

S5. Compare $P^{(l+1)}$ with $P^{(l)}$. If they are close enough, then STOP, else increase l by 1 and GOTO S3.

For a proof of the minimization in step S4 see Bezdek [21].

The closeness of two fuzzy partitions is evaluated in step S5 using a distance. A good choice is the distance induced by the L_∞ norm, *i.e.,* if the larger difference between two consecutive fuzzy membership degrees is smaller than certain ε, then stop the procedure.

As discussed above, the choice for the geometrical shape of the classes influences the prototypes and the relationships leading to the minimization of $J(P^{(l)}, \cdot)$ in step S3. For instance, let us assume that the classes have spherical shape. This leads to the prototypes L_i being points in the space $\mathbf{R}^s$ of the data set. Consequently, we define the dissimilarity as

$$D(x^j, L_i) = d(x^j, L_i)^2 = \left\| x^j - L_i \right\|^2$$

where d is the Euclidean distance in the space $\mathbf{R}^s$. It follows that the prototypes L_i that minimize $J(P^{(l)}, \cdot)$ at step S3 above are determined as follows [21]:

$$L_i = \frac{\sum_{j=1}^{n} A_i(x^j)^m \cdot x^j}{\sum_{j=1}^{n} A_i(x^j)^m}.$$

For examples of other geometrical prototypes, see Bezdek et al. [22] and Höppner et al. [13].

Following the results discussed by Dunn [20] and Bezdek [21], the method described above converges to a local optimum. Let us remember that our problem is to fuzzify a given crisp partition, such that it matches the best cluster structure of the data. The local optimum found in the vicinity of the initial crisp partition, as determined by this method, is, actually, the desired result.

Prediction step: assign fuzzy values to new items

Consider a data set $X = \{x^1, \ldots, x^n\}$, with $x^j \in \mathbf{R}^s$ for all values of j. Consider known the fuzzy partition $P = \{A_1, \ldots, A_c\}$ corresponding to the cluster structure of X as determined in the previous step. Consider a data set $Y = \{x^{n+1}, \ldots, x^{n+p}\}$ we need to predict their fuzzy membership degrees to the given fuzzy partition P. The procedure is an extension of the procedure indicated in [21].

Under the same assumptions as above, we will proceed as follows:

S1. Set l = 0;

S2. Initialize fuzzy partition $P^{(0)} = \{A_1, \ldots, A_c\}$ to be the given fuzzy partition P;

S3. Compute the prototypes L_i that minimize $J(P^{(l)}, \cdot)$;

S4. Compute the fuzzy partition $P^{(l+1)}$ that minimizes $J(\cdot, L)$, as follows:

$$A_i^{(l+1)}(x^j) = \frac{1}{\sum_{k=1}^{c} \left(\frac{D(x^j, L_i)}{D(x^j, L_k)} \right)^{\frac{1}{m-1}}}, \text{for } j = n+1, \dots, n+p.$$

S5. Compare $P^{(l+1)}$ with $P^{(l)}$. If they are close enough, then STOP, else increase *l* by 1 and GOTO S3.

At the step S4, only the fuzzy membership degrees of the data items in *Y* are updated. The values of the data items in *X* are not touched, as we are interested in predicting the fuzzy memberships for the newly available data items. The same discussion on the choice of prototypes *L* and dissimilarity *D* as above is, of course, valid at this point and the same reasoning on the local optima as above is also valid.

REFERENCES

1. D.L. Massart, B.G.M. Vandeginste, S.N. Deming, Y. Michotte, L. Kaufman, Chemometrics: a Textbook, Elsevier, Amsterdam, **1988**.
2. J.W. Einax, H. Zwanziger, S. Geiß, Chemometrics in Environmental Analysis, John Wiley & Sons Ltd, Chichester, UK, **1997**.
3. R.G. Brereton, Applied Chemometrics for Scientists, John Wiley & Sons Ltd, Chichester, UK, **2007**.
4. M. Otto, Chemometrics. Statistics and Computer Application in Analytical Chemistry, third ed., Wiley-VCH, Weinheim, **2017**.
5. R.G. Brereton, Chemometrics: Data Driven Extraction for Science, second ed., John Wiley & Sons Ltd, Chichester, UK, **2018**.
6. B. Nisbet, G. Miner, K. Yale, Handbook of Statistical Analysis and Data Mining Applications, second ed., Academic Press, Elsevier Inc., **2018**.
7. C. Bouveyron, G. Celeux, T.B. Murphy, A.E. Raftery, Model-based Clustering and Classification for Data Science, University Printing House, Cambridge, **2019**.
8. S. Borra, R. Thanki, N. Dey, Satellite Image Analysis: Clustering and Classification, Springer Nature, Singapore Pte Ltd., **2019**.
9. C. Hennig, M. Meila, F. Murtagh, R. Rocci, R. (Eds), Handbook of Cluster Analysis, CRC Press, Boca Raton, New York, **2016**.
10. L.A. Zadeh, *Inf. Control,* **1965**, *8*, 338–353.
11. D.A. Simovici, C. Djeraba, Mathematical Tools for Data Mining: Set Theory, Partial Orders, Combinatorics, second ed., Springer-Verlag, London, UK, **2014**.
12. D.H. Rouvray, (Ed), Fuzzy Logic in Chemistry, Academic, San Diego, **1997**.

13. F. Höppner, R.K. Klawonn, R. Kruse, T. Runkler, Fuzzy Cluster Analysis: Methods for Classification, Data Analysis and Image Recognition, John Wiley & Sons, Chichester, UK, **1999**.
14. H.F. Pop, C. Sârbu, O. Horovitz, D. Dumitrescu, *J. Chem. Inf. Comput. Sci.*, **1996**, *36*, 465-482.
15. Y. Jin, L. Wang, (Eds), Fuzzy Systems in Bioinformatics and Computational Biology, Springer-Verlag, Heidelberg, **2009**.
16. T-C.T. Chen, K. Honda, Fuzzy Collaborative Forecasting and Clustering, Springer Nature, Switzerland AG, **2020**.
17. P. Mirti, V. Zelano, R. Aruga, E. Ferrara, L. Appolonia, *Archaeometry,* 32 **1990**, *32*, 163-175.
18. C. Sârbu, K. Zehl, J.W. Einax, *Chemometr. Intell. Lab. Syst.*, **2007**, *86*, 121-129.
19. C. Sârbu, J. W. Einax, *Anal. Bioanal. Chem.*, **2008**, *390*, 1293–1301.
20. J.C. Dunn, *J. Cybern.*, **1973**, *3*, 32–57.
21. J.C. Bezdek, Pattern Recognition with Fuzzy Objective Function Algorithms, Plenum Press, New York, **1981**.
22. J.C. Bezdek, C. Coray, R. Gunderson, J. Watson, *SIAM J. Appl. Math.*, **1981**, *40*, 339–372.
23. D.P.S. Peacock, Pottery in the Roman World: an Ethnoarchaeological Approach, Long Man, New York, **1982**.
24. J.T. Peña, Roman Pottery in the Archaeological Record, Cambridge University Press, UK, **2007**.
25. A. Shiyab, A. Al-Shorman, N. Turshan, M. Tarboush, F. Alawneh, A. Rahabneh, *J. Archaeol. Sci. Rep.*, **2019**, *25*, 100–115.